A REAL-TIME ADAPTIVE THRESHOLDING FOR VIDEO CHANGE DETECTION

Chang Su and Aishy Amer

Concordia University, Electrical and Computer Engineering, Montréal, Québec, Canada
Email: {chan_su, amer}@ece.concordia.ca

ABSTRACT

A real-time adaptive non-parametric thresholding algorithm for change detection is proposed in this paper. Based on the estimation of the scatter of regions of change in a difference image, a threshold of each image block is computed discriminatively, then the global threshold is obtained by averaging all the thresholds for image blocks. The block threshold is calculated differently for regions of change and background. Experimental results show the proposed thresholding algorithm performs well for change detection with high efficiency.

Index Terms— Image processing, object detection, image segmentation

1. INTRODUCTION

Change detection is widely used in video processing and analysis [1, 2, 3]. Image differencing followed by thresholding is a popular method for change detection [1, 2, 4, 5, 6]. Thresholding plays a pivotal role in such change detection methods.

Many thresholding methods have been proposed in literatures, however, few of them are specific to change detection. Thresholding methods can be classified into gray-level distribution based [7, 8] and spatial properties based [4, 6, 9]. After evaluating many thresholding methods for change detection, Rosin *et. al.* [4, 5] recommend three thresholding methods: Euler-number [6, 9], Poisson-noise modeling [4], and Kapur method [7]. The Euler-number thresholding is based on the assumption that the number of regions of change in a difference image will tend to be stable over a wide range of threshold values. The Poisson-noise modeling thresholding is based on the assumption that observations (number of pixels over a specific threshold) in an image usually follow a Poisson distribution. The Kapur thresholding is entropy based.

These three thresholding methods perform well for change detection. However, the loads of computation of the Euler-number thresholding and Poisson-noise modeling thresholding are high and not suitable in real-time. In addition, the Poisson-noise modeling thresholding is sensitive to its parameter, the window size. The Euler method tends to underthreshold some images. The Kapur thresholding is sensitive to the noise level and underthreshold a difference image.

This work is supported, in part, by the Natural Science and Engineering Research Council (NSERC) of Canada.

In this paper, we propose a real-time adaptive thresholding for change detection that overcomes the shortages of these reference thresholding methods. Section 2 describes the proposed thresholding algorithm. Section 3 presents experiments and comparison to the reference thresholding methods. Section 4 concludes this paper.

2. THE PROPOSED ALGORITHM

The proposed non-parametric algorithm computes a threshold of each block of an image adaptively based on the scatter of regions of change (ROC) and averages all thresholds for image blocks to obtain the global threshold.

First, the output D_n of a change detection at time instant n, is divided into K equal-sized blocks. Then a ROC scatter estimation algorithm (Sec. 2.1) is applied, where each image block $W_k, k = \{1, 2, \cdots, K\}$, is marked either as containing ROC, denoted W_k^r, or not containing ROC, denoted W_k^b. The threshold T_k^b of a W_k^b is computed by a noise statistical-testing algorithm (Sec. 2.2). The threshold T_k^r of a W_k^r is computed by a noise-robust thresholding method (Sec. 2.3). That is, the threshold T_k of a W_k in D_n is defined as

$$T_k = \begin{cases} T_k^r & \text{of} \quad W_k^r \\ \\ T_k^b & \text{of} \quad W_k^b. \end{cases} \tag{1}$$

Finally, the global threshold T_n of a difference image D_n is

$$T_n = \frac{1}{K} \sum_{k=1}^{K} T_k \tag{2}$$

Since size and velocity of objects, noise, local changes in videos may affect the histogram of a W_k, the first moment of histogram is used to estimate the scatter of ROC making the estimation (Eq.3 and 4) adaptive to these characteristics. We also account for noise (Eq.5) and local changes (Eq.10)

2.1. ROC Scatter Estimation

The ROC in D_n are, in general, scattered over the K image blocks. Let i be a pixel in D_n that varies between 0 and 255. i is high in ROC which are caused by strong changes such

as motion or significant illumination changes and is low in non ROC which are caused by slight changes such as noise or slight illumination changes. We use the first moment, m_k, of the histogram of each image block W_k as a measure for determining if an image block contains ROC.

$$m_k = \sum_{i=1}^{g_{max}} i \cdot F_i \tag{3}$$

where F_i is the frequency of gray-level $i = \{1, 2, \cdots, g_{max}\}$ and g_{max} is the maximum gray-level in the image block. If m_k of W_k is greater than a threshold T_m, the image block is regarded as a block containing ROC, and marked as W_k^r, otherwise, it is marked as W_k^b, i.e.,

$$W_k = \begin{cases} W_k^b & : \quad m_k \leq T_m \\ W_k^r & : \quad m_k > T_m \end{cases} \tag{4}$$

$\{m_k\}$ may vary greatly under different video conditions. We propose, therefore, to adaptively determine T_m as follows. Non-zero pixels in image blocks without ROC are in general caused by noise, illumination changes, or background movement. Those factors usually affect an image globally thus m_k for different W_k^b should be similar to each other. To find T_m, we first compute the m_k of each block and then descending sort the m_k values. A straight line between the first bin and the last filled bin is then drawn. T_m is selected to maximize the perpendicular distance between the line and the sorted first moment curve (see Fig.1 where we use relative $\{m_k\}$.)

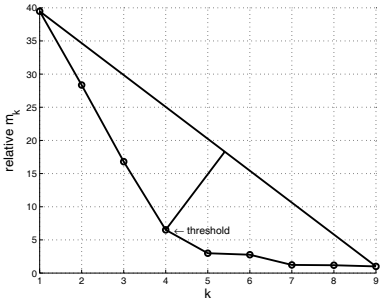

Fig. 1. An example of adaptive m_k thresholding ($K = 9$).

2.2. Thresholding in background (Non ROC)

To account for video noise, we model the noise as a Gaussian distribution with zero mean $N(0, \sigma_\nu^2)$ with σ_ν^2 as the noise variance. In such a case, the noise in the difference image obtained by image differencing followed by taking absolute value can be modeled as $2N(0, 2\sigma_\nu^2)$ [4]. Since a linear function of a Gaussian random variable is also a Gaussian random variable [10], let $\sigma_D = \sqrt{2}\sigma_\nu$, the noise of a difference image can be modeled as a new Gaussian distribution $N(\mu_D, \sigma_D^2)$, where μ_D and σ_D^2 are the mean and variance of the noise in a difference image, respectively, and μ_D is usually zero.

For image blocks without ROC, non-zero pixels are usually caused by noise. So based on the noise model above, for each W_k^b we can find a T_k^b, where the pixels in W_k^b are highly-probable lower than T_k^b. The gray-level T_k^b is a reasonable threshold for W_k^b, i.e., the probability that the pixels in an image block W_k^b are lower than T_k^b should satisfy

$$P[X \leq T_k^b] > p_h \tag{5}$$

where $X = W_k^b(i, j)$ is the gray-level of a pixel at location (i, j) in W_k^b and p_h is a high probability value. Then

$$P[X \leq T_k^b] = \int_{-\infty}^{T_k^b} \frac{1}{\sqrt{2\pi}\sigma_k} e^{-\frac{(x-\mu_k)^2}{2\sigma_k^2}} \, dx \tag{6}$$

where μ_k and σ_k^2 are the mean and variance of gray-level in image block W_k^b, respectively. Let $t = \frac{x-\mu_k}{\sigma_k}$, we get

$$P[X \leq T_k^b] = \Phi\left(\frac{T_k^b - \mu_k}{\sigma_k}\right) > p_h \tag{7}$$

where $\Phi(\cdot)$ is the cumulative distribution function (cdf) of standard normal distribution. To estimate p_h, using the standard normal distribution table [10], we have $\Phi(2.8) = 0.9975$. Because the cdf of a random variable is a non-decreasing function [10], $P[X \leq T_k^b] > 0.9975$ means $\frac{T_k^b - \mu_k}{\sigma_k} > 2.8$, i.e., $T_k^b > \mu_k + 2.8\sigma_k$. The threshold of an image block without ROC is, therefore defined as

$$T_k^b = \mu_k + c \cdot \sigma_k \tag{8}$$

where c is a varying coefficient (Eq.9) to improve the robustness to noise, illumination changes, or background movement. The coefficient c is determined adaptively based on the min-max ratio of m_k, $r_m = \frac{m_{min}}{m_{max}}$, where m_{min} and m_{max} are minimum and maximum of all m_k in D_n. Because noise, illumination changes, and background movement in an image can significantly increase the probability of the occurrence of a high gray-level in W_k^b, m_{min} for such an image increases greatly. This leads the ratio r_m increasing too. So r_m is a good measure to adaptively estimate c as follows (Fig.2).

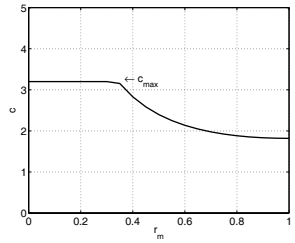

Fig. 2. Adjusting rate function of c vs. r_m.

$$\begin{aligned} c_r &= \frac{1}{r_m} e^{r_m} - \alpha \\ c &= \begin{cases} c_{max} & : \quad c_r > c_{max} \\ c_r & : \quad \text{otherwise} \end{cases} \end{aligned} \tag{9}$$

where c_{max} is the maximum value of c determinted by Eq.7, and α is a constant experimentally set to 0.9.

2.3. Thresholding In ROC

For each image block W_k^r containing ROC, we propose the local-change adaptive thresholding. First, the histogram of each W_k^r is computed and divided into L equal partitions, and the most frequent gray-level $g_{f_l}, l = \{1, 2, \cdots, L\}$, in each histogram partition is fixed (Fig.3). Then the average gray-level μ_k of W_k^r is computed and the threshold T_k^r of W_k^r is obtained by averaging the sum of all g_{f_l} and μ_k, i.e.,

$$T_k^r = \frac{\sum_{l=1}^{L} g_{f_l} + \mu_k}{L+1} \tag{10}$$

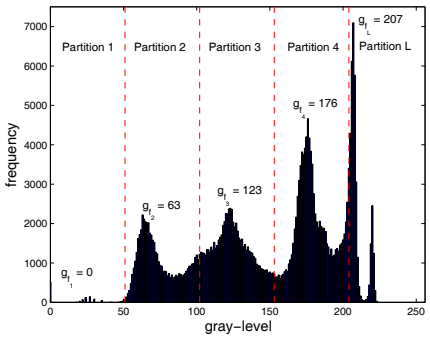

Fig. 3. An example of fixing the most frequent gray-level in each histogram partation ($L = 5$).

3. EVALUATION AND COMPARISON

To test the proposed algorithm, the change detection method in [3] is used in to create difference images $\{D_n\}$. The evaluation is performed by applying the proposed method as well as the three thresholding methods recommended in [5, 4], i.e., Euler, Poisson, and Kapur thresholding, to videos containing different contents. Since the Otsu thresholding [8] is widely used, it is also included in our comparison.

Sample results are shown for indoor "Hall" (300 frames of size 352×248), indoor "Meeting room" (300 frames of size 320×240), and outdoor "Survey" (1000 frames of size 320×240). In our simulations, $K = 9$ and $L = 5$. Fig.4 shows sample results where we use change detection with background subtraction. As can be seen, the proposed method outperforms the Euler and Kapur method, and its performance is similar to Poisson method.

To test the noise robustness of the proposed method, the 25 dB PSNR noisy "Survey" is used. In Fig.5, we note that

(a) (b) (c) (d) (e)

Fig. 4. Comparison with "Hall" (top) and "Survey" (bottom). (a) original images I_{148} and I_{50} (b)—(e) masks by proposed, Poisson, Euler, and Kapur methods, respectively.

the Poisson and the proposed methods have similar performance and Euler method underthresholds the noisy images. The Kapur method performs poorly for noisy videos.

(a) (b) (c) (d) (e)

Fig. 5. Comparison with 25 dB noisy "Survey". (a) I_{50} (b)—(e) masks by proposed, Poisson, Euler, and Kapur methods.

The Poisson and Euler methods are sensitive to spatial properties of an image, e.g., the object size or the range of gray-level. Fig. 6 shows comparison using a QCIF size "Hall". Poisson and Euler methods break down for many frames. Fig. 7 shows the binary results using different change detection methods. As we can see, Poisson method seriously overthresholds and Otsu underthresholds.

We also test the proposed and the reference methods using successive frame-differencing change detection. Experimental results (e.g., Fig.8) show that Poisson, Euler, and Kapur methods tend to overthreshold.

(a) (b) (c) (d) (e)

Fig. 6. Comparison with QCIF "Hall". (a) I_{120} (b)—(e) masks by proposed, Poisson, Euler, and Kapur methods, respectively.

In addition, an objective measure, the Jaccard similarity coefficient (JC), using ground truth [1, 5] is used where the higher a measure is, the better the thresholding is. The JC measures for 25 dB noisy "Hall" is shown in Fig.9 where the proposed method outperforms the Euler and Kapur methods, and its performance equal the Poisson method.

Based on visual and objective evaluation, we conclude that 1) the proposed method has significantly better performance than the gray-level distribution based methods [7, 8],

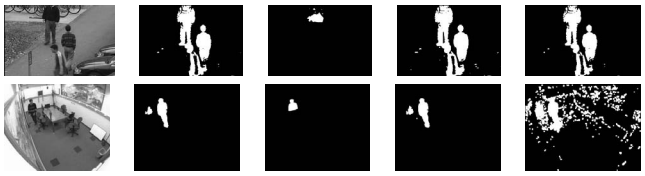

(a) (b) (c) (d) (e)

Fig. 7. Comparison with "Survey" (top) and "Meeting room" (bottom) for variations of CD methods. (a) I_{100} and I_{234} (b)—(e)masks by proposed, Poisson, Euler, and Otsu methods, respectively.

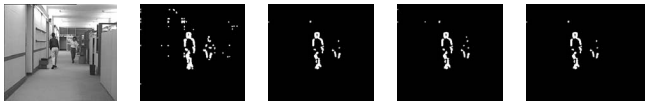

(a) (b) (c) (d) (e)

Fig. 8. Comparison with "Hall" using successive frame differencing. (a)I_{148} (b)—(e) masks by proposed, Poisson, Euler, and Kapur methods, respectively.

2) the proposed method is more stable than the more advanced, Euler and Poisson, methods [4, 6, 9], 3) overall the proposed method outperforms all the reference methods followed by Poisson, Euler, Kapur and Otsu method, 4) Otsu method is not suitable for change detection as it may give extremely low objective measure and noisy output (see also [11]).

Finally, the average computation time of the proposed method is over 27 times lower than the Euler method, and over 8 times lower than the Possion method.

4. CONCLUSION

A real-time adaptive non-parametric thresholding method for video object change detection is proposed in this paper. Noise and local changes are taken into account. Based on the estimation of the scatter of regions of change of a difference image, a threshold of each image block is computed discriminatively. The global threshold is the average of all thresholds of image blocks. Both the visual assessment and the objective evaluation show that the proposed method clearly outperforms the gray-level distribution based methods and is more stable than the spatial properties based methods. The efficiency of the proposed method is much higher than the spatial properties based methods.

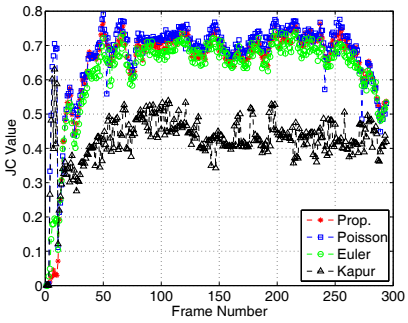

Fig. 9. JC measure for noisy 25 dB "Hall".

5. REFERENCES

[1] R. J. Radke, S. Andra, O. A-Kofahi, and B. Roysam, "Image change detection algorithms: a systematic survey," *IEEE Transactions On Image Processing*, vol. 14, no. 3, pp. 294–307, 2005.

[2] D. Zhang and G. Lu, "Segmentation of moving objects in image sequence: a review," *Circuits Systems Signal Processing*, vol. 20, no. 2, pp. 143–183, 2001.

[3] A. Amer and E. Dubois, "Memory-based spatio-temporal real-time object segmentation," *Proc. SPIE Int. Symposium on Electronic Imaging, Conf. on Real-Time Imaging*, vol. 5012, pp. 10–21, 2003.

[4] P. L. Rosin, "Thresholding for change detection," *Computer Vision and Image Understanding*, vol. 86, pp. 79–95, 2002.

[5] P. L. Rosin and E. Ioannidis, "Evaluation of global image thresholding for change detection," *Pattern Recognition Letters*, vol. 24, pp. 2345–2356, 2003.

[6] P. L. Rosin and T. Ellis, "Image difference threshold strategies and shadow detection," *In Proc. British Machine Vision Conference*, pp. 347–356, 1995.

[7] J. Kapur, P. Sahoo, and A. Wong, "A new method for gray-level picture thresholding using the entropy of histogram," *Computer Vision, Graphics Image Process*, vol. 29, no. 3, pp. 273–285, 1985.

[8] N. Otsu, "A threshold selection method from gray-level histogram," *IEEE Trans. System, Man and Cybernetics*, vol. 19, pp. 62–66, 1979.

[9] A. Pikaz and A. Averbuch, "Digital image thresholding based on topological stable state," *Pattern Recognition*, vol. 29, pp. 829–843, 1996.

[10] A. Leon-Garcia, *Probability and Random Processes For Electrical Engineering*, Addison-Wesley Publishing Company Inc., second edition, 1994.

[11] H. Lee and R. Park, "Comments on "an optimal multiple threshold scheme for image segmentation"," *IEEE. Trans. On Systems, Man, And Cybernetics*, vol. 20, no. 3, pp. 741–742, 1990.